XLI CILAMCE
XLI Ibero-Latin American Congress on Computational Methods in Engineering
16-19 November, 2020 FOZ DO IGUAÇU PARANÁ – BRAZIL

SURROGATE BASED OPTIMIZATION OF FUNCTIONALLY GRADED PLATES USING PSO AND DE

Leonardo G. Ribeiro[1], Jonatas M. F. C. Martins[1], Evandro Parente Junior[1], A. Macário C. de Melo[1]

[1]*Laboratório de Mecânica Computacional e Visualização (LMCV), Departamente de Engenharia Estrutural e Construção Civil, Universidade Federal do Ceará*
Campus do Pici, Bloco 728, 60440-900, Ceará-Brazil
leonardoribeiro@alu.ufc.br, cacaujonatas9@gmail.com, evandro@ufc.br, macario@ufc.br

Abstract. Optimization procedures are often employed in the design of functionally graded structures to achieve a superior efficiency. Thus, this paper aims at comparing the Particle Swarm Optimization and the Differential Evolution algorithms when applied to the optimization of FG plates. The optimization is carried out using the Isogeometric Analysis to evaluate the structural responses and Radial Basis Functions are used as a surrogate modeling technique to lower the computation cost. A Sequential Approximate Optimization approach is used to improve the surrogate model during the optimization process. The two optimization algorithms will also be compared in terms of accuracy and computational efficiency.

Keywords: Differential Evolution, Particle Swarm Optimization, Functionally Graded Plates, Surrogate modeling.

1 Introduction

Functionally Graded Materials (FGM) are a class of composite where the material properties may vary continuously in a given direction. Optimization techniques can be used to explore the potential of these materials. This way, the volume fraction of each material, as well as design parameters such as the structure thickness, may be defined to minimize a given objective function, while still respecting some constraints.

In structural optimization, it is common for researchers to prefer heuristic algorithms over mathematical programming optimization methods due to their capability of avoiding local minima. These algorithms are also usually easier to employ, since there is no need to compute the gradients of objective and constraint functions. Recent papers can also be found advising the use of Particle Swarm Optimization (PSO) over the Genetic Algorithm (GA), since most optimization problems regarding FG structures deal with continuous variables [1]. Indeed, many researchers make use of the PSO to optimize FG structures, with great success [1, 2].

In that matter, another commonly used heuristic algorithm proposed to deal with a continuous design space is the Differential Evolution (DE) [3]. Recently, this heuristic has also been applied in the optimization of complex FG structures, achieving good results [4]. Furthermore, papers which focused on the comparison between PSO and DE usually find out that DE is superior both in terms of accuracy and convergence speed [5]. However, a direct comparison regarding FGM has not been made yet.

This paper presents the comparison between PSO and DE formulations when applied to the optimization of FG structures. A Sequential Approximate Optimization approach will be adopted, where a surrogate model is used to perform an approximated but efficient assessment of a given costly function [6]. Then, the surrogate model is continuously improved by the addition of new sampling points via the maximization of the Expected Improvement (EI) [7, 8]. This maximization procedure is often performed by an heuristic algorithm due to the nature of the EI function, which may be highly multimodal [8]. Once again, both the DE and the PSO will be compared to define which heuristic algorithm performs best in these cases.

This paper is organized as follows. In Section 2 the Functionally Graded Plates (FGP) are decribed in more detail. In Section 3 the focus is given to the optimization algorithms used, and the operators and parameters of both the DE and the PSO are introduced. In Section 4 the SAO approach is explained, and surrogate model building and assessment of the Expected Improvement are discussed. The results are presented in Section 5, and in Section

6 the main conclusions are discussed.

2 Functionally Graded Plates

In this paper, the focus is given to FG plates made of two materials, usually a ceramic and a metal, whose proportion varies through thickness. The volume fraction variation may be controlled by a power-law function [9] defined as:

$$V_c(z) = \left(\frac{1}{2} + \frac{z}{h}\right)^p, \quad V_m(z) = 1 - V_c(z), \quad -\frac{h}{2} \leq z \leq \frac{h}{2} \tag{1}$$

where V_c is the volume fraction of a ceramic material, varying in the plate thickness h, V_m is the volume fraction of a metallic material, and p is an exponent controlling the volume fraction variation.

In order to enhance the design flexibility, B-Splines can be used to define the material gradation [2, 10]:

$$V_c(\xi) = \sum_{i=1}^{n_{cp}} B_{i,p}(\xi)\, V_{c,i}, \quad V_m(\xi) = 1 - V_c(\xi) \quad \xi \,\epsilon\, [0,1] \tag{2}$$

where n_{cp} is the number of control points, $V_{c,i}$ is the fraction of the ceramic volume of the i-th control point, $B_{i,p}(\xi)$ is the corresponding B-Spline base, p is the base degree and ξ is the parametric coordinate. The definition of the base $B_{i,p}(\xi)$ requires a node vector, composed of non-negative and non-decreasing parametric values, delimited by the parametric interval in which the B-Spline is defined. Given a node vector $\Xi = [\xi_1, \xi_2, ..., \xi_{n+p+1}]$, the functions of the B-Spline base are evaluated by the Cox-de Boor recursive formula [2, 10].

The effective properties of a FG structure depends both on the properties of the constituents and the proportion of each material at each point. The evaluation of the effective properties of the material requires the use of an appropriate homogenization scheme [11]. The simplest approach is the Rule of Mixtures (RoM) [9], where the effective material property (P) is given by the weighted average of the constituent properties. Another widely used approach is the Mori-Tanaka scheme, where the structure, formed by a material m, is assumed to be reinforced by spherical particles from material c.

3 Optimization algorithms

The Particle Swarm Optimization (PSO) was initially developed in 1995, proposed by Kennedy and Eberhart [12]. This heuristic, based on swarm intelligence, quickly received a surge in popularity due to its excellent results in continuous spaces, both in terms of accuracy and convergence speed. This paper will make use of a version presented in Barroso et al. [13].

The PSO starts by generating N_p random particles in a fixed bound-constrained space. Each particle j is defined by their position $\mathbf{x}_j^{(0)}$ and velocity $\mathbf{v}_j^{(0)}$, where the superscript denotes the current iteration. Thus, at each iteration, the particle moves based on its velocity:

$$\mathbf{x}_j^{(i+1)} = \mathbf{x}_j^{(i)} + \mathbf{v}_j^{(i+1)}, \text{ where } \mathbf{v}_j^{(i+1)} = w\,\mathbf{v}_j^{(i)} + c_1\, r_1 \left(\mathbf{x}_{p,j}^{(i)} - \mathbf{x}_j^{(i)}\right) + c_2\, r_2 \left(\mathbf{x}_{g,j}^{(i)} - \mathbf{x}_j^{(i)}\right) \tag{3}$$

where w represents the inertia of the particle, while c_1 and c_2 are the cognitive and social factors, $\mathbf{x}_{p,j}^{(i)}$ is the best position obtained by particle j during the optimization and $\mathbf{x}_{g,j}^{(i)}$ is the best position obtained by a particle on the neighborhood of j.

The neighborhood of a particle may be defined by different topologies. Kennedy and Eberhart [12] initially proposed the use of a Global topology, where all particles are considered in the neighborhood. However, it was realized that this choice may suffer from premature convergence in multimodal problems [14]. Thus, the use of the Square (or von Neumann) or the Ring topology may offer a better accuracy, although at a loss of efficiency due to a slower convergence speed [13, 14].

To further improve PSO exploration capabilities, Barroso et al. [13] proposed the use of a mutation operator. Thus, after a new position is calculated in iteration i, each variable k of each particle j has a small probability p_{mut} of mutating to a new random value, respecting the bound constraints.

Differential evolution (DE) was initially developed by Storn and Price [3] and is widely known as an efficient and robust algorithm for searching for a global optimal solution in a continuous domain [4, 5]. An important characteristic is the small number of control parameters: the scale factor F and the crossover probability C_r.

The DE starts by randomly generating an initial population of N_p members within a search domain, each of these candidate solutions being an m-dimensional vector of design variables. After the evaluation of each

individual, the mutation operator takes place, controlled by the scale factor F. In the original DE formulation, this operator is given by [15]:

$$v_{j,i} = x_{j,r0} + F\left(x_{j,r1} - x_{j,r2}\right) \tag{4}$$

where $x_{j,r0}$, $x_{j,r1}$ and $x_{j,r2}$ are candidate solutions, $r0$, $r1$ and $r2$ are natural numbers chosen at random in the range $[1, N_p]$ and $v_{j,i}$ is the mutated vector. This formulation is known as Rand/1, since the base vector $x_{j,r0}$ is chosen randomly and only one difference vector is considered. Since its initial development, many improvements were proposed by different researchers. Many different operators to carry out the differential mutation can be listed, but two of the most adopted ones are the Best/1 and the Current-to-best/1, respectively [15]:

$$v_{j,i} = x_{j,best} + F\left(x_{j,r1} - x_{j,r2}\right), \text{ and } v_{j,i} = x_{j,i} + F\left(x_{j,best} - x_{j,i}\right) + F\left(x_{j,r1} - x_{j,r2}\right) \tag{5}$$

where $x_{j,best}$ is the best design found during the optimization process. Although the Best/1 approach is able to provide good results, it is a common issue for it to present a very localized search. This paper will use a jitter approach [15], where F presents a small random variation each time a variable is mutated. This approach is known as Best/1 with jitter.

A binomial crossover is then carried out to increase the diversity of the population, controled by the crossover probability C_r. After evaluating the final mutated population, the selection is employed: if the i-th mutated design is worse than the i-th individual in the previous generation, the latter does not get replaced [15].

For both algorithms, the iterative process keeps repeating until a stopping criteria is met, usually related to a maximum number of iterations It_{max} or a maximum number of consecutive iterations with no considerable improvement It_{stall}.

4 Sequential Approximate Optimization

To improve computational efficiency, this paper will also make use of a Sequential Approximate Optimization (SAO) approach, where, at each step, a response surface is built based on a small set of sampling points. Then, an optimization procedure is performed to define a new point that should be added to the sample set. Once again, the process continues until a stopping criteria is met.

An important step on the process is the definition of the initial sample. Since no information about the function behavior is known *a priori*, it is a good practice to spread these points uniformly in the design space [6]. A simple but commonly used approach is the Latin Hypersquare, which can inexpensively generate random well-distributed samples in the design space. An improved approach will be used where 20 different samples will be generated, and the one where the minimum distance between two points is maximized is selected to perform the model building [6, 10]. In this paper, the size of the initial sample will be defined as $n_i = 5\,m$, where m is the number of design variables considered on a given problem.

The response surface is built using the Radial Basis Functions (RBF) [6], while the new sampling point is defined in each iteration by the maximization of the Expected Improvement (EI) [7, 8]. The following subsections describe these steps in detail, which were employed in FG optimization problems in recent work with great success [10].

4.1 Radial Basis Functions

Given a set of sampling points c_j, a RBF surrogate model for a function which exact responses are given by $\mathbf{y}$ is defined as:

$$\hat{y}(\mathbf{x}) = \sum_{j=1}^{n} w_j\, \psi_j(||\mathbf{x} - \mathbf{c}_j||), \text{ or } \hat{\mathbf{y}} = \mathbf{w}^T \boldsymbol{\psi} \tag{6}$$

where w_j represents the j-th basis weight, n is the number of sampling points and ψ_j the basis function relative to the j-th sampling point ($\mathbf{c}_j$). In this work, the Gaussian basis function will be used to interpolate different sampling points:

$$\psi(r) = \exp\left(-r^2/\sigma^2\right) \tag{7}$$

where σ is known as the basis' width. Many papers have proposed different ways of estimating this parameter [8, 10]. Ribeiro et al. [10] present a comparison between some of these methods, showing that the 5-Fold Cross-Validation (5-FCV) can provide a great accuracy, while still being the most efficient method between the ones tested. In this paper, this approach will be employed.

Finally, the weight vector $\mathbf{w}$ may be defined by interpolation, considering that $\hat{\mathbf{y}} = \mathbf{y}$ on the sampling points. Thus:

$$\boldsymbol{\Psi}\mathbf{w} = \mathbf{y}, \text{ where } \Psi_{ij} = \psi_j(||\mathbf{c}_i - \mathbf{c}_j||) \tag{8}$$

where $\mathbf{\Psi}$ is the so-called Gram matrix.

4.2 Expected Improvement

Each iteration of the SAO algorithm ends with the addition of a new sampling point, in an attempt of improving the surrogate model accuracy over the global optima region. In this paper, this new point will be defined by maximizing the Expected Improvement (EI) of a given surrogate model. The EI is an error-based metric based on theory of Gaussian processes [6] and may be evaluated as:

$$E[I(\mathbf{x})] = (y_{min} - \hat{y}(\mathbf{x}))\left[\frac{1}{2} + \frac{1}{2}\text{erf}\left(\frac{y_{min} - \hat{y}(\mathbf{x})}{\hat{s}\sqrt{2}}\right)\right] + \frac{\hat{s}}{\sqrt{2\pi}}\exp\left[\frac{-(y_{min} - \hat{y}(\mathbf{x}))^2}{2\hat{s}^2}\right] \tag{9}$$

where y_{min} is the best objective function currently on $\mathbf{y}$ and $\hat{s}^2$ denotes the estimated mean squared error [6]:

$$\begin{aligned} \hat{s}^2(\mathbf{x}) &= \hat{\sigma}^2\left[1 - \boldsymbol{\psi}^T\mathbf{\Psi}^{-1}\boldsymbol{\psi} + \frac{\left(1 - \mathbf{1}^T\mathbf{\Psi}^{-1}\boldsymbol{\psi}\right)^2}{\mathbf{1}^T\mathbf{\Psi}^{-1}\mathbf{1}}\right] \\ \hat{\sigma}^2 &= \frac{(\mathbf{y} - \mathbf{1}\hat{\mu})^T\mathbf{\Psi}^{-1}(\mathbf{y} - \mathbf{1}\hat{\mu})}{n},\ \hat{\mu} = \frac{\mathbf{1}^T\mathbf{\Psi}^{-1}\mathbf{y}}{\mathbf{1}^T\mathbf{\Psi}^{-1}\mathbf{1}} \end{aligned} \tag{10}$$

Here, $\hat{\sigma}^2$ and $\hat{\mu}$ are the the maximum likelihood estimate for the variance and the mean, respectively.

In a constrained optimization problem, there are two possibilities. If a constraint is cheap and easy to evaluate, it is not necessary to use a surrogate model to approximate it. Thus, the constraint is evaluated and, if violated, the $E[I(\mathbf{x})]$ of an unfeasible individual is set to 0 [8]. If the constraint assessment is computationally costly, it may be approximated by a surrogate model. However, since the surrogate provides only an estimate of the real function, it is not trivial to determine if a certain individual is feasible or not. Thus, the Probability of Feasibility can be used to assist in the handling of constraints. A parameter $F(\mathbf{x})$ may be evaluated by [16]:

$$F(\mathbf{x}) = \begin{cases} \dfrac{1}{2} + \dfrac{1}{2}\text{erf}\left(\dfrac{g_{min} - \hat{g}(\mathbf{x})}{\hat{s}(\mathbf{x})}\right) & \text{, if erf}\left(\dfrac{g_{min} - \hat{g}(\mathbf{x})}{\hat{s}(\mathbf{x})}\right) = 1 \\ 2 - \text{erf}\left(\dfrac{g_{min} - \hat{g}(\mathbf{x})}{\hat{s}(\mathbf{x})}\right) & \text{, if } 0 < \text{erf}\left(\dfrac{g_{min} - \hat{g}(\mathbf{x})}{\hat{s}(\mathbf{x})}\right) < 1 \\ 0 & \text{, otherwise} \end{cases} \tag{11}$$

where g_{min} is the constraint bound, which will be always taken as 0 in this paper. Then, the constrained expected improvement of a given point is evaluated by:

$$CE[I(\mathbf{x})] = F(\mathbf{x})\, E[I(\mathbf{x})] \tag{12}$$

Each SAO iteration consists of the RBF model building and the definition of the new sampling point via maximization of the EI. Thus, in each iteration one new point is added to the sample. In this paper, it will be assumed that the maximum number of points is $n_{max} = 3\,n_i$, where n_i is the number of points in the initial sample [8]. Alternatively, if the algorithm offers no improvement for 10 consecutive iterations, the optimization process ends.

5 Numerical examples

In this section, two different problems will be optimized both in a conventional manner and using the SAO approach. Different types of PSO and DE will be tried out to define which one performs best.

For PSO, three different swarm topologies will be tested: Square, Ring and Global. For DE, also three different types of differentiation will be employed: Rand/1, Current-to-best/1 and Best/1 with jitter. Using a conventional algorithm, it was assumed that $N_p = 50$, $It_{max} = 50$ and $It_{stall} = 20$. The default PSO parameters employed are $w = 0.72$, $c_1 = c_2 = 1.50$ and $p_{mut} = 2\%$, while the default DE parameters are $F = 0.85$ and $C_r = 80\%$. For the SAO algorithm, $It_{max} = 500$ is used due to the cheaper evaluation cost of the objective function. Since the optimization methods are non-deterministic, 10 runs will be performed for each method.

Comparisons will be performed in terms of the average Normalized Root Mean Squared Error ($\overline{\text{NRMSE}}$) with the global optimum [10]. Also, the average Wall-Clock Time ($\overline{\text{WCT}}$) will be used to evaluate the efficiency of an approach. On SAO approaches, the average total number of high fidelity sampling points evaluated $\overline{n}_p$ will be shown. All numerical computations were performed on a computer with a core i9-9820X CPU of 3.30 GHz clock speed and 128 GB of RAM. No parallelization procedure was used.

Table 1 presents the properties of the materials used in those examples.

Table 1. Material properties.

Material	E (GPa)	ν	ρ (kg/m^3)
Al	70.00	0.3000	2707
SUS304	201.04	0.3000	8166
Al_2O_3	380.00	0.3262	3800
Si_3N_4	348.43	0.2400	2370

5.1 Example 1

The first example deals with a two-dimensional problem proposed by Correia et al. [9]. The maximization of the fundamental frequency of a SUS304/Si_3N_4 square plate with $a = 0.50$ m is performed. Effective properties are defined via the Rule of Mixtures. The design variables are the plate thickness h, defined in the domain $[0.005, 0.06]$ m, and the exponent p of the power-law function, defined in the domain $[0.2, 10]$. Two constraints are considered, defining an upper and a lower bound for the fundamental frequency ω. A 16×16 cubic NURBS mesh is employed. The optimization problem may be stated as:

$$\begin{cases} \text{maximize} & \omega(\mathbf{x}) = \omega(p, h) \\ \text{subjected to} & g_1(\mathbf{x}) = \omega(\mathbf{x})/8000 - 1 \leq 0 \quad \text{and} \quad g_2(\mathbf{x}) = 1 - \omega(\mathbf{x})/3000 \leq 0 \end{cases} \tag{13}$$

Figure 1(a) presents how $\omega(\mathbf{x})$ behaves in the design space. The feasible region is given by the space between the two horizontal planes, which represent the two constraints.

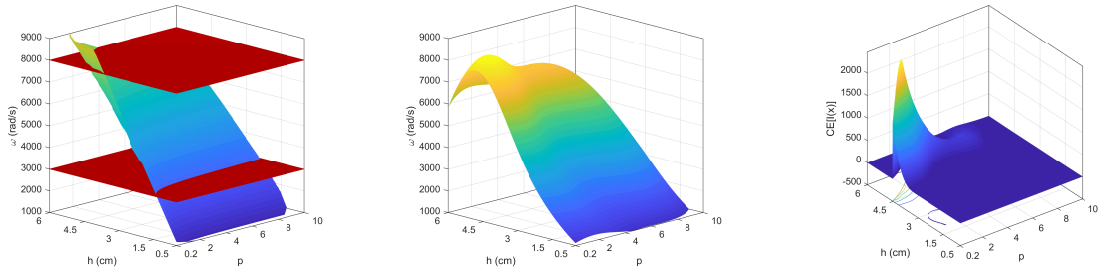

(a) Objective function surface mesh (b) RBF prediction (c) Constrained EI surface

Figure 1. Behavior of $w(\mathbf{x})$ and initial SAO surfaces on Example 1

This problem has a smooth and unimodal response function. Thus, it is expected for both algorithms to perform well. On the other hand, the problem has multiple optimum designs, all laying in the plane where $\omega(\mathbf{x}) = 8000$ rad/s. This is the surface that will be maximized in the case of the conventional optimization.

Figures 1(b) and 1(c) present the RBF prediction and $CE[I(\mathbf{x})]$ surface obtained using 10 sampling points. In this problem, the constraints are also approximated by a surrogate model. Thus, the Constrained EI should be maximized to choose a new sampling point, according to Eq. (11). Indeed, its optimum region seems to be close to the global optimum shown in Figure 1(a). In each SAO iteration, a different surface, similar to the one shown in Fig. 1(c), needs to be maximized. The heuristic algorithms must be able to perform consistently well to provide the expected efficiency.

Table 2 presents the results in terms of the average NRMSE found by each algorithm and their Wall-Clock Time. Overall, all the results were very good. Using a conventional optimization, all approaches achieved the global optimum with great accuracy, presenting a Wall-Clock Time of nearly 1500 s. The DE/Best/1 with jitter approach was the most efficient, achieving a $\overline{\text{WCT}}$ of 1065 s, as it seems to present a faster convergence. Regarding the SAO approaches, even though these did not achieve the global optimum as accurately, their efficiency is outstanding, with a Wall-Clock Time of less than 30 s in most cases, being 97% faster than the conventional methods. Here, the DE presented slightly lower $\overline{\text{WCT}}$s.

Table 2. Results found for the Example 1.

Algorithm/Type	Conventional optimization		SAO		
	$\overline{\text{NRMSE}}$	$\overline{\text{WCT}}$	$\overline{\text{NRMSE}}$	$\overline{\text{WCT}}$	$\overline{n}_p$
PSO/Global	0.00%	1447 s	0.28%	30 s	28
PSO/Square	0.00%	1509 s	0.50%	30 s	28
PSO/Ring	0.00%	1549 s	0.52%	27 s	26
DE/Rand/1	0.00%	1412 s	0.40%	23 s	26
DE/Current-to-best/1	0.00%	1529 s	0.55%	24 s	26
DE/Best/1 with jitter	0.00%	1065 s	0.39%	24 s	27

5.2 Example 2

This example was proposed by Do et al. [2] and deals with the maximization of buckling load N_{cr} of a Al/Al_2O_3 square plate with $a/h = 10$. In this case, effective properties are defined via the Mori-Tanaka scheme. Also, the material gradation through the thickness is defined by B-Spline with 13 control points. Since the gradation is supposed to be symmetric at the mid-plane, there are 7 design variables, each defined in the domain $[0, 1]$. Also, a constraint related to the maximum percentage of ceramic $V_{c,max} = 35\%$ is considered. In this case, since the constraint has an easy and cheap evaluation, there is no need to approximate it by a surrogate model. Instead, the constraint is exactly evaluated and, if a given design is unfeasible, its Expected Improvement is set to 0 [8], as discussed in Section 4.2. Thus, the surrogate model is used only to approximate the objective function. A 16×16 cubic NURBS mesh is employed. The optimization problem is stated as:

$$\begin{cases} \text{maximize} & \lambda(\mathbf{x}), \text{ where } \lambda = N_{cr}\, a/D_m \text{ and } D_m = E_m\, h^3/[12(1-{\nu_m}^2)] \\ \text{subjected to} & \dfrac{1}{h}\int_{-h/2}^{h/2} V_c(\mathbf{x})\, dz - 0.35 \leq 0 \end{cases} \tag{14}$$

where E_m and ν_m refers to the metal properties.

Do et al. [2] found a $\lambda_{opt} = 12.241$. In our case, the optimum value is slightly lower, since this work employs a First-order Shear Deformation Theory [10], and $\lambda_{opt} = 11.638$. Table 3 presents the results for both the conventional optimization and the SAO approach. Here, $\overline{\lambda}_{opt}$ defines the average λ found. Regarding the conventional optimization, it is clear that, in this problem, the DE performed much better in terms of accuracy. The best overall approach was the Best/1 with jitter, which presented a better efficiency as well. Once again, the SAO approaches did manage to greatly improve the optimization algorithm efficiency while still being able to find designs very close to the optima. Concerning the comparison between heuristics, there is not a noticeable difference between results found. Average results between different optimizations were similar.

Table 3. Results found for the Example 2.

Algorithm/Type	Conventional optimization			SAO			
	$\overline{\lambda}_{opt}$	$\overline{\text{NRMSE}}$	$\overline{\text{WCT}}$	$\overline{\lambda}_{opt}$	$\overline{\text{NRMSE}}$	$\overline{\text{WCT}}$	$\overline{n}_p$
PSO/Global	11.326	2.68%	1912 s	11.576	0.53%	25 s	48
PSO/Square	11.635	0.02%	2082 s	11.610	0.24%	26 s	48
PSO/Ring	11.634	0.04%	2348 s	11.547	0.78%	25 s	48
DE/Rand/1	11.608	0.26%	2472 s	11.591	0.40%	27 s	48
DE/Current-to-best/1	11.638	0.00%	2543 s	11.579	0.51%	25 s	47
DE/Best/1 with jitter	11.638	0.00%	1965 s	11.562	0.66%	26 s	48

6 Conclusion

A comparison between two meta-heuristic algorithms was performed to assess which one performs better in the optimization of functionally graded plates. Thus, three Particle Swarm Optimization (PSO) variants and three Differential Evolution (DE) variants were put to test and compared both in terms of accuracy and efficiency. The comparison was carried out considering the conventional approach based on the evaluation of the plate responses using a numerical method (IGA) and the Sequential Approximate Optimization (SAO) approach based on a RBF surrogate and the EI as infill criterion.

Regarding the conventional approach, the DE seems to be the more accurate algorithm, being able to consistently achieve the lowest errors. The highest overall efficiency was found by the Best/1 with jitter approach, where lower Wall-Clock Times can be found. On the other hand, concerning the SAO approach, the difference between meta-heuristics is not as noticeable. However, DE was slightly more efficient than PSO.

Acknowledgements

The financial support by CNPq (Conselho Nacional de Desenvolvimento Científico e Tecnológico) is gratefully acknowledged.

Authorship statement. The authors hereby confirm that they are the sole liable persons responsible for the authorship of this work, and that all material that has been herein included as part of the present paper is either the property (and authorship) of the authors, or has the permission of the owners to be included here.

References

[1] Ashjari, M. & Khoshravan, M., 2014. Mass optimization of functionally graded plate for mechanical loading in the presence of deflection and stress constraints. *Composite Structures*, vol. 110, pp. 118–132.

[2] Do, D., Lee, D., & Lee, J., 2019. Material optimization of functionally graded plates using deep neural network and modified symbiotic organisms search for eigenvalue problems. *Composites Part B: Engineering*, vol. 159, pp. 300–326.

[3] Storn, R. & Price, K., 1997. Differential evolution - a simple and efficient heuristic for global optimization over continuous spaces. *Journal of Global Optimization*, vol. 11, n. 4, pp. 341–359.

[4] Truong, T. T., Nguyen-Thoi, T., & Lee, J., 2019. Isogeometric size optimization of bi-directional functionally graded beams under static loads. *Composite Structures*, vol. 227, pp. 111259.

[5] Iwan, M., Akmeliawati, R., Faisal, T., & Al-Assadi, H. M., 2012. Performance comparison of differential evolution and particle swarm optimization in constrained optimization. *Procedia Engineering*, vol. 41, pp. 1323–1328.

[6] Forrester, A. I. J., Sobester, A., & Keane, A. J., 2008. *Engineering design via surrogate modelling: a practical guide*. Wiley.

[7] Jones, D. R., Schonlau, M., & Welch, W. J., 1998. Efficient global optimization of expensive black-box functions. *Journal of Global Optimization*, vol. 13, pp. 455–492.

[8] Sobester, A., Leary, S. J., & Keane, A. J., 2005. On the design of optimization strategies based on global response surface approximation models. *Journal of Global Optimization*, vol. 33, pp. 31–59.

[9] Correia, V. M. F., Madeira, J. A., Araújo, A. L., & Soares, C. M. M., 2018. Multiobjective optimization of ceramic-metal functionally graded plates using a higher order model. *Composite Structures*, vol. 183, pp. 146–160.

[10] Ribeiro, L. G., Maia, M. A., Parente Jr.., E., & Melo, A. M. C. D., 2020. Surrogate based optimization of functionally graded plates using radial basis functions. *Composite Structures*, vol. 252.

[11] Shen, H. S., 2009. *Functionally graded materials: Nonlinear analysis of plates and shells*. CRC Press.

[12] Kennedy, J. & Eberhart, R., 1995. Particle swarm optimization. *Proceedings of ICNN'95 - International Conference on Neural Networks*.

[13] Barroso, E. S., Parente Jr., E., & Melo, A. M. C. D., 2016. A hybrid pso-ga algorithm for optimization of laminated composites. *Structural and Multidisciplinary Optimization*, vol. 55, n. 6, pp. 2111–2130.

[14] Bratton, D. & Kennedy, J., 2007. Defining a standard for particle swarm optimization. *2007 IEEE Swarm Intelligence Symposium*.

[15] Price, K. V., Storn, R. M., & Lampinen, J. A., 2005. *Differential Evolution: A pratical approach to Global Optimization*. Springer.

[16] Tutum, C. C., Deb, K., & Baran, I., 2014. Constrained efficient global optimization for pultrusion process. *Materials and Manufacturing Processes*, vol. 30, n. 4, pp. 538–551.